Kinetics and Catalysis, Vol. 46, No. 5, 2005, pp. 641–659. Translated from Kinetika i Kataliz, Vol. 46, No. 5, 2005, pp. 682–700.

Physicochemical Principles of the Synthesis of Porous Composite Materials through the Hydrothermal Oxidation of Aluminum Powder

S. F. Tikhov*, V. E. Romanenkov, V. A. Sadykov*, V. N. Parmon*, and A. I. Rat'ko*****

** Boreskov Institute of Catalysis, Siberian Division, Russian Academy of Sciences, Novosibirsk, 630090 Russia*

*** Institute for the Advanced Training and Retraining of Personnel in New Areas of the Development of Engineering, Technology, and Economics, Belarussian State Technical University, Minsk, Belarus*

**** Institute of General and Inorganic Chemistry, Belarussian Academy of Sciences, Minsk, 270072 Belarus*

Received September 24, 2004

Abstract—The main versions of the synthesis of a new class of porous cermet materials such as Al_2O_3/Al, MO_x/Al_2O_3/Al, and $M^1/MO_x/Al_2O_3$/Al and ceramic composites on their basis were analyzed. These ceramic composites were prepared through the stage of the hydrothermal oxidation of aluminum powder and were designed for catalytic and adsorption processes. Equations that express the dependence of the apparent density of the resulting composite on the density of the initial powder mixture, on the concentration of the powdered active component, and on the conversion of aluminum are given. It was found that the formal kinetics of aluminum oxidation with water at 100°C can be described by the Kolmogorov–Erofeev equation. The results were compared with data obtained in an autoclave at higher temperatures and steam pressures. The synthesis parameters that affect the total pore volume and the specific surface area of aluminum oxide obtained from aluminum powder were determined. For the case of the transfer of soluble components from an autoclave to a press mold, the molar coefficients of this process were calculated. The texture peculiarities of composites were analyzed. The texture exhibited a polymodal character with developed micropore, mesopore, and ultramacropore structures, which are responsible for the high permeability of granulated composites. Factors affecting the mechanical properties of metal ceramics were studied. The catalysts and products of composite materials were exemplified.

INTRODUCTION

Current trends in the development of the chemical industry include the miniaturization of chemical reactors and the intensification of heat- and mass-transfer processes with an increase in the efficiency of chemical processes. In this context, a number of special requirements are imposed on the properties of highly porous catalytic materials. Thus, the catalysts should exhibit a required mechanical strength at a high porosity. Specific chemical properties, which are responsible for high catalytic activity and selectivity, should be combined with the chemical and thermal stability of catalysts under conditions of real reaction media. Moreover, in a number of cases, specially shaped products should be prepared in order to provide for the optimum dynamic properties of a gas or liquid flow.

The development of new high-porosity materials occurs in various areas. However, as a rule, multiphase systems should be used due to the combination of various and often mutually exclusive physicochemical properties of materials. Metal ceramics or cermets can serve as an example of these materials. Cermets are composite materials containing one or more metals in combination with one or more ceramic phases (oxides, carbides, or nitrides) [1]. The properties of these materials are intermediate between the properties of porous metals obtained by powder metallurgy (as a rule, they exhibit high mechanical strength, plasticity, thermal conductivity, and electric conductivity) and the properties of highly dispersed porous ceramics (mainly oxide), which exhibit high thermal and chemical resistance and hardness.

The preparation of cermets by the oxidation of aluminum metal has found expanding applications in the synthesis of supports and catalysts [2–4], sensor devices [5], and filter elements [6], although energy consumption for the production of the main raw materials is relatively high (high-temperature electrolysis, sputtering for powder formation, rolling for foil formation, etc.). As a result, aluminum oxide with an unusual texture, mechanical, and chemical properties is formed; Al_2O_3 prepared by the classical techniques of colloid chemistry is devoid of these properties.

The hydrothermal synthesis of porous Al_2O_3/Al cermets based on the chemical interaction of water or steam with aluminum powder placed in a special die occupies an important place [7]. Unlike other methods of aluminum oxidation [8–10], this synthesis immediately affords granulated composites rather than powders. A procedure for the preparation of these cermets

0023-1584/05/4605-0641 © 2005 MAIK "Nauka/Interperiodica"

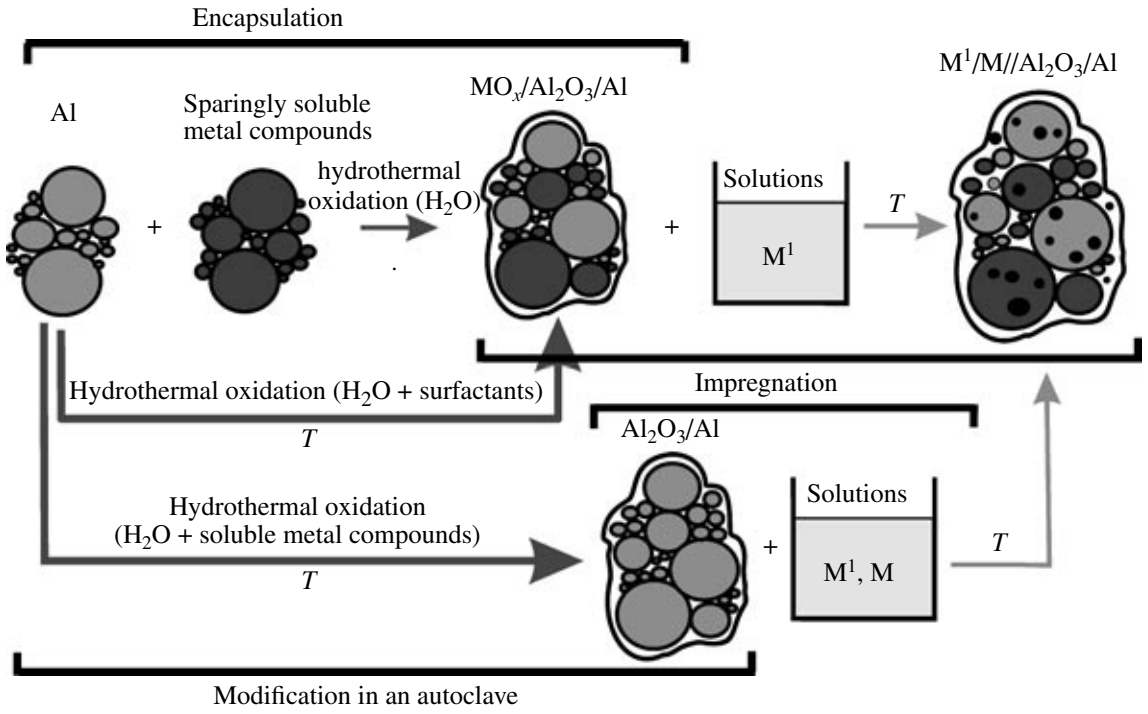

Fig. 1. Main versions of the synthesis of porous metal oxide composites with the use of aluminum powder.

is based on a combination of techniques used in colloid chemistry and powder metallurgy. These composite (or ceramic on the complete conversion of aluminum) materials also occupy an intermediate place between well-known granulated porous ceramic materials and permeable powder materials in terms of pore structure and mechanical properties. According to Andreeva [1], porous cermets based on Al_2O_3 belong to metal oxide oxide-matrix isotropic discrete composite materials. The aim of this work was to summarize the results of a comparison between synthetic procedures and a study of the most important properties of the new class of porous materials.

1. MAIN METHODS FOR THE SYNTHESIS OF POROUS COMPOSITES BASED ON Al_2O_3/Al FROM ALUMINUM POWDER

The synthesis of cermets is based on the chemical interaction of aluminum powder with water or steam, the formation of aluminum hydroxides, and the thermal decomposition of these hydroxides to alumina. In the simplest case, a mechanically strong composite is formed in which residual aluminum particles are uniformly distributed in a common porous shell of Al_2O_3. Figure 1 illustrates the main versions of the synthesis of cermets. The hydrothermal oxidation of aluminum powder with water or steam is the simplest method of the synthesis of composites. In this case, the texture properties and composition of cermets are controlled by varying the conditions of hydrothermal oxidation: temperature, process time, and steam pressure.

The texture modification of cermets can also be performed in an autoclave with the use of either soluble organic substances (surfactants) or the solutions of inorganic substances to obtain a more complex composite: $M^1O_x/Al_2O_3/Al$. Because not only aluminum is oxidized in this case but other processes occur as well, it is more appropriate to designate this method as hydrothermal synthesis rather than hydrothermal oxidation. Cermets of this kind can be synthesized by the traditional impregnation of a previously prepared Al_2O_3/Al composite with appropriate solutions in order to additionally introduce oxides and metals into the composite. However, in these modes of synthesis, the pore volume decreases, because the free space of an aluminum oxide matrix is filled by the component introduced from solution. Complex composites can also be synthesized by the encapsulation of sparingly soluble oxides mixed with aluminum powder. In this case, both the micropore and the macropore structures can be considerably developed (because of the intrinsic microporosity of the oxide additive and changes in the packed density of powder particles, respectively). These composites can also be additionally modified with, for example, platinum-group metals, by impregnation.

Table 1. Effect of additives on the properties of $MO_x/Al_2O_3/Al$ composites (PA-4 aluminum powder)

MO_x	z	y'	α	V_α^*, cm^3/g	δ_α^*, g/cm^3	z''	δ_0	δ_α, g/cm^3	ρ_{MO_x}, g/cm^3	V_α, cm^3/g
–	–	0.19	0.11	0.39	1.34	0	1.19	1.31	–	0.40
CaO	0.04	0.26	0.16	0.25	1.60	0.05	1.05	1.43	3.40	0.31
La_2O_3	0.05	0.21	0.12	0.32	1.51	0.06	1.09	1.40	6.50	0.34
MgO	0.06	0.31	0.19	0.23	1.75	0.07	0.80	1.49	3.60	0.29
TiO_2	0.01	0.28	0.17	0.29	1.57	0.01	1.01	1.39	3.80	0.33

Notes: z is the fraction of the MO_x oxide in $MO_x/Al_2O_3/Al$ in terms of stoichiometric oxides according to chemical analysis data.

$z'' = m_{MO_x}/m_{Al}^0$, where m_{MO_x} is the oxide amount in the cermet formed after hydrothermal oxidation in a corresponding solution and thermal treatment.

y' and α are the fraction of Al_2O_3 in the cermet and the conversion of aluminum, respectively (evaluated from X-ray diffraction data).

V_α and δ_α are the specific pore volume and apparent density of cermets, respectively (calculated values); experimental values are marked with asterisks.

ρ_{MO_x} is the true density of oxides according to published data [13, 14].

δ_0 is the packed density of aluminum powder.

2. FACTORS RESPONSIBLE FOR THE APPARENT DENSITY OF PELLETIZED COMPOSITES

The apparent density of composites is an important technological characteristic, determining the density of catalyst beds. At the same shape of pellets and a given reactor volume, a denser catalyst can provide a greater unit volume activity even at the same specific activity of samples.

For Al_2O_3/Al composites, the relationship between the apparent density of pellets (δ_α), the bulk density of aluminum powder (δ_0), and the conversion of aluminum (α) is determined by the following equation [10]:

$$\delta_\alpha = (\alpha X_0 + 1)\delta_0, \quad (1)$$

where $X_0 = \dfrac{m_{Al_2O_3} - m_{Al}}{m_{Al}} = 0.89$ is the relative mass change upon the complete conversion of aluminum into oxide. Equation (1) is valid for a rigid press mold, in which the volume of a solid remains constant without a considerable carryover of the substance from the press mold. Evidently, the apparent density of granules increases because the free space is filled with the resulting aluminum oxide (or hydroxide).

For the more complex composites $MO_x/Al_2O_3/Al$, on the fulfillment of the above conditions and with the retention of the phase and chemical composition of the oxide additive after the synthesis of the composite, the value of δ_α depends on the MO_x content of the initial mixture (z') and other parameters [11]:

$$\delta_\alpha = \delta_0[1 + \alpha X_0(1 - z')], \quad (2)$$

where δ_0 characterizes the bulk density of the mixture containing a certain amount of the additive. From Eq. (2), it follows that the dependence of the apparent density of the composite on the conversion of aluminum weakens as the concentration of the oxide additive is increased.

The situation becomes much more complicated if a powdered additive is carried away from the die to the autoclave under hydrothermal conditions. In this case, to predict changes in the apparent density, not only the value of z' but also the dependence of the additive content of the composite (z) on the reaction conditions of hydrothermal oxidation and on the design of the die, which can be determined only experimentally, should be known. In this case, the equation has the following form [11]:

$$\delta_\alpha = \delta_0\frac{(1 - z')(1 + \alpha X_0)}{1 - z}. \quad (3)$$

The modification of a cermet from solution in the course of hydrothermal oxidation in an autoclave results in an inverse phenomenon: an increase in the weight as a result of aluminum oxidation, substance transfer to the die, and deposition in the pores of the composite (analogously to an impregnation procedure). In this case, the apparent density increases in accordance with the following relation:

$$\delta'_\alpha = \delta_0(1 + \alpha X_0 + z''), \quad (4)$$

where z'' is the weight fraction of MO_x with respect to the starting mixture containing aluminum powder. This value characterizes the transfer of the substance from solution to the die ($m_{MO_x} = z''m_{Al}^0$).

A comparison between the calculated and experimental apparent densities demonstrated that the results were consistent [11, 12]. It is most likely that the difference between these values, which increased with increasing fraction of an oxide additive, was due to the shrinkage of pellets on the thermal decomposition of hydroxides. Table 1 summarizes calculated data for the case of transfer from solution. A comparison with experimental values (δ_α^*) demonstrates the applicabil-

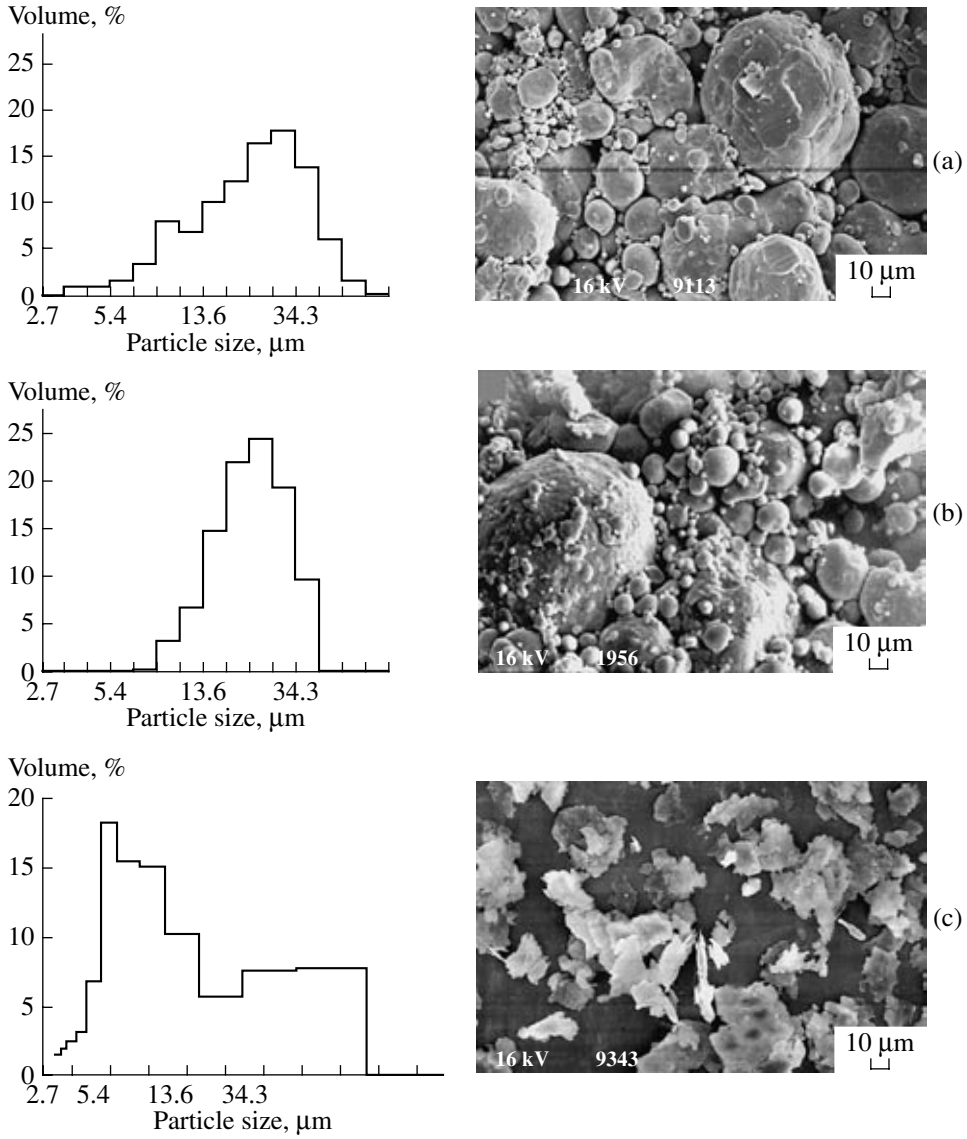

Fig. 2. Particle sizes and electron micrographs of aluminum powders: (a) PAHP (TU 48–5–172–77), (b) PA-4 (GOST 6058–73; OOO SUAL PM), and (c) silver-like aluminum powder (GOST 5499–71).

ity of the proposed equations to the prediction of the apparent density of composite pellets. The systematic deviation of the calculated values of δ_α from experimental ones is most likely due to an underestimated value of the bulk density of a mixture, which was determined in special experiments under conditions different from those on filling the press mold.

3. BULK DENSITY OF THE POWDER CHARGE

From Eqs. (1)–(4), it follows that the properties of cermets essentially depend on not only the conversion of aluminum but also the properties of the powder mixture, which depend on the bulk density (δ_0) or porosity (ε_0). In the most general form, the relationship between the apparent density and porosity of granulated solids is expressed by the following equation [14]:

$$\varepsilon = 1 - \delta/\rho = V\rho/(1 + V\rho) = V\delta, \qquad (5)$$

where ρ is the true density of the material, and V is the specific pore volume.

The bulk density of powders depends on many parameters. In the absence of a strong mechanical action (pressing or vibration compaction), the particle size distribution of a powdered substance can also affect the bulk density [15]. For example, the bulk density of a PAHP aluminum powder (~1.5), which has a wider particle size distribution, is greater than that of a PA-4 powder (~1.2) at a similar average particle size (Fig. 2). The bulk density increases with decreasing average particle size (at a wide particle size distribu-

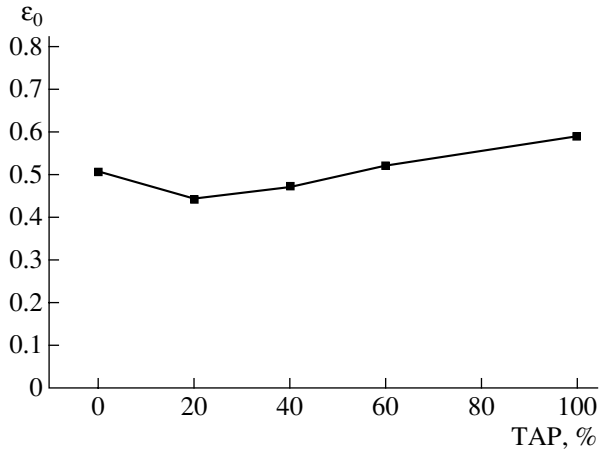

Fig. 3. Dependence of the porosity of a mixture containing a thermochemical activation product (TAP) and aluminum powder (PA-4) on composition.

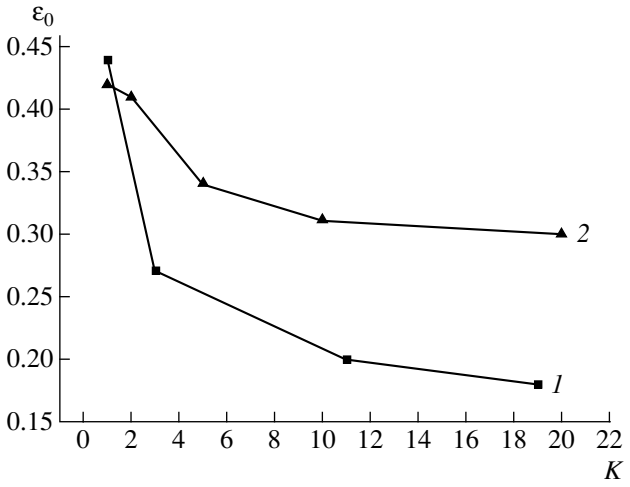

Fig. 4. Dependence of porosity on the value of $K = d_1/d_2$ for a bidisperse blend containing 50% coarsely dispersed phase: (*1*) Al + ZrFeH and (*2*) published data [16, 17].

tion). The so-called shape factor [9], which characterizes the deviation of particle shape from an ideal sphere [15], is of considerable importance. Thus, the bulk density of a silver-like powder that consists of flat partially aggregated particles (~0.3) is much lower than that of PA-4 and PAHP powders with almost ideal spherical particles (Fig. 2). The height of the column in the die can also affect both the average density and the inhomogeneity of bulk density along the bed height.

Peronius and Sweeting [16] estimated the minimum porosity of monodisperse spherical particles (ε_0) at ~0.42. The values of ε_0 found in our experiments (under a minimum mechanical action by percussion) for spherically shaped aluminum particles were greater (~0.44 for PAHP and ~0.53 for PA-4); this is indicative of a loose random packing of particles in a mixture.

Additional problems occur on mixing aluminum powder with other components for the synthesis of catalysts or modified supports. It is well known that the porosity of bidisperse systems that consist of equally shaped particles with different sizes depends on the weight fraction of the coarse portion (z') with particle size d_1 in the mixture at various ratios between the particle sizes of two fractions ($K = d_1/d_2$) and passes through a minimum whose depth increases with K [15, 16]. A decrease in the porosity with increasing coarsely dispersed fraction is consistent with a model in which small particles are arranged in the spaces between coarse particles. After reaching a minimum, small particles, which completely filled the spaces between coarse particles, separated coarse particles to result in an increase in the porosity [15]. Indeed, for a mixture of aluminum powder (true density, 2.76; average particle size, 24 μm) and a powdered thermochemical activation product based on amorphous aluminum hydroxide (true density, 2.68; average particle size, 9 μm), the porosity plotted as a function of the mixture composition passes through a minimum (Fig. 3). However, on the average, the porosity is higher than that in the ideal case.

Figure 4 shows the dependence of porosity on the value of K at equal concentrations (50%) of the components of a bidisperse mixture. To construct this graph, we used published data [15, 16] for an ideal case. We obtained an analogous curve for a bidisperse blend of a PAHP aluminum powder and a ZrFeH intermetallic hydride (synthesized at the Topchiev Institute of Petrochemical Synthesis, Russian Academy of Sciences, Moscow) with a similar composition. The constituents of this mixture significantly differ in true density (2.7 and 6.75, respectively) and particle shape. We found that, in this case, the porosity dramatically decreases with K, especially in the range K = 1–3 (Fig. 4). This fact should be taken into consideration in the prediction of the properties of resulting composites.

Changes in the packed density (porosity of a mixture) are even more different from the idealized function with the use of powdered oxide additives having a true density close to the density of aluminum powder (2.4–4.5) with the average particle size varied over a wide range (from 7.7 to 21.9 μm). Thus, it was found that the mixing of the PA-4 powder with 20% oxide additive resulted in a decrease in the packed density (Table 1). An analogous behavior was observed after the introduction of coarse fractions in the production of granulated supports by so-called wet methods [17, 18]. The considerable intrinsic porosity of oxide additives, which is characteristic of aluminum and magnesium oxides, can be responsible for the decrease in δ_0. The particles of an oxide additive can also be predominantly arranged immediately between aluminum particles to separate particles in the mixture because of the imperfect shapes and surface roughness of additive particles or electrostatic effects. Thus, some properties of the resulting cermets can be regulated even at the stage of

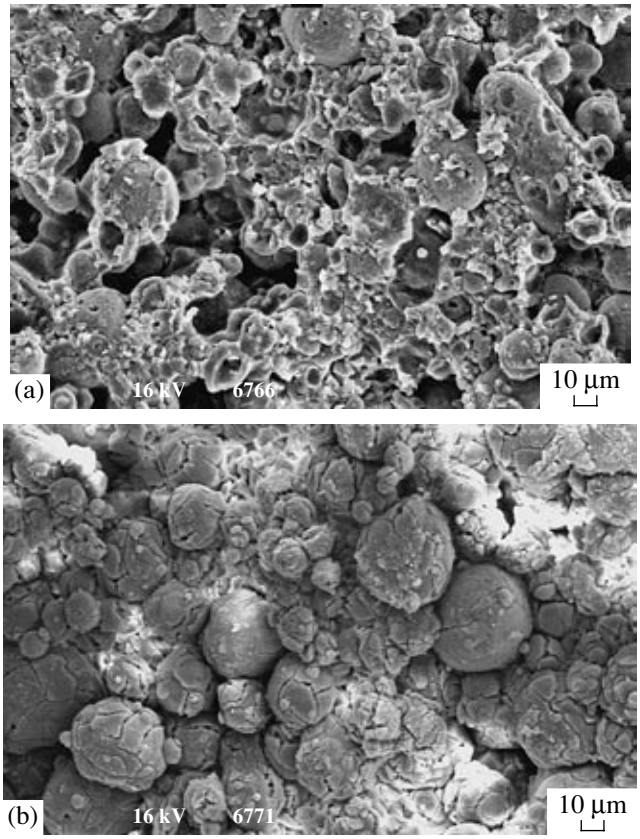

Fig. 5. Electron micrographs of Al_2O_3/Al composites prepared from PAHP after hydrothermal treatments under various conditions followed by calcination in air. Conversion: (a) 38.7 and (b) 58.4%.

formation of a powder mixture (mixing and placing powders in a die).

4. HYDROTHERMAL SYNTHESIS OF COMPOSITES

As noted above, hydrothermal treatment results not only in aluminum oxidation but also in side processes. Hydrothermal oxidation is one of the most important stages in the formation of composites based on aluminum powder. The electrochemical dissolution of aluminum, the formation of aluminate ions (the simplest building material required for the production of an $Al(OH)_3$/Al or AlOOH/Al composite by hydroxide crystallization from solution), and the formation of cermet compositions occur at this stage. In the simplest case, when only the hydrothermal oxidation of aluminum takes place without transferring the solid-phase reaction products from the die, the conversion of aluminum and the alumina content of the composite (y) are interrelated as follows [10]:

$$y = \frac{\alpha(X_0 + 1)}{\alpha X_0 + 1}; \quad \alpha = \frac{y}{1 + X_0(1 - y)}. \qquad (6)$$

Knowing the dependence of the conversion of aluminum (α) on treatment time, temperature, water vapor pressure, specific reactivity of aluminum, etc., we can not only control the composition of the resulting cermets but also regulate the micropore and macropore structure and mechanical properties of composites and the texture properties of Al_2O_3. Thus, the average ultramicropore size of cermets considerably decreased with the conversion of PAHP aluminum (Fig. 5).

At small values of Al_2O_3 (hydrothermal oxidation temperatures lower than 100°C), the oxidation of aluminum with water was a topochemical reaction that consisted of a number of consecutive steps [20, 21]:

(1) an induction period, during which the hydration and dissolution of an oxide film occurred with the formation of a complex ion and three hydroxyl groups:

$$Al_2O_3 \cdot xH_2O + 6H_2$$
$$\longrightarrow [Al(H_2O)_6]^{3+} + 3OH^-;$$

(2) a step of reaction acceleration due to an increase in the reactive aluminum surface (the acceleration of oxide film dissolution was associated with an increase in the pH of water [19]);

(3) a step of decay, when the aluminum surface was coated with the reaction product, and the process changed to the diffusion region; the pH of water remained unchanged at the last two steps.

Special experiments performed under conditions of intense stirring (200 rpm) of an ASD-1 powder allowed us to determine the kinetic parameters of the reaction near the point of inflection at various Al/H_2O weight ratios (from 1/20 to 1/800 g/g); this is also of importance for understanding the process of hydrothermal oxidation. We found that the reaction rate, which was determined from the release of gaseous hydrogen, decreased with water content (Fig. 6a). The plot of α as a function of time exhibits two segments (intervals) with a clear inflection of curve. Moreover, we found that the pH value of water noticeably increased in the first interval and remained almost constant in the second interval (Fig. 6b); this behavior is somewhat different from that observed previously [20, 21]. The value of pH in a horizontal segment decreased with increasing concentration of H_2O. It is likely that surface activation processes due to the hydration of an oxide film and the growth of a reactive surface interfered with each other as the value of α increased at the initial segment and the reaction occurred in an autocatalytic mode. At a constant pH, when the reaction changed to the diffusion region, the rates of consumption and formation of OH groups were approximately equal and the difference between pH values mainly depended on the Al/H_2O ratio.

The concentration of hydroxyls in a microvolume adjacent to the reaction surface is much higher than that in solution, and it is responsible for the rate of chemical reaction. To calculate the concentration of OH groups,

we used the Fick diffusion law (assuming a stationary character of transfer in layer δ)

$$C_1 = \frac{w_{kin}\delta}{D} + C_2, \quad (7)$$

where w is the experimentally found rate of hydrogen release calculated per square meter of the reaction surface; C_1 is the concentration of hydroxyls in a microvolume adjacent to the reaction surface; and C_2 is the measured concentration of hydroxyls in a macrovolume (Fig. 6b). Calculated data demonstrated that the concentration of hydroxyls in a near-surface layer was higher than that in the macrovolume by an order of magnitude.

The simplest description of the kinetics of aluminum oxidation under the given conditions was obtained using the Kolmogorov–Erofeev equation [24, 25], which has the following logarithmic form:

$$\log[-\ln(1-\alpha)] = n\log kt, \quad (8)$$

where k and n are constants.

The experimental data suggest that the value of k decreased with decreasing Al/H_2O, whereas the apparent order of reaction with respect to water and the time taken to reach the point of inflection (τ_{kin}) increased (Table 2).

Another procedure for increasing α and regulating the composition of composite materials consists in the thermal dehydration of the products of hydrothermal oxidation with the formation of aluminum oxide [22, 23]. Thus, in the thermal decomposition of bayerite, the effective pore radius increased (from 1.9–2.0 to 2.8–3.1 nm) and the sorption pore volume increased more than two times. As a result, the permeability of a porous shell on the surface of aluminum particles increased and diffusion limitations were removed; the conversion of aluminum upon repeated hydrothermal treatment increased.

For additionally increasing the reactivity of aluminum, oxidation was performed in an autoclave. This allowed one to increase both the temperature and the pressure of water vapor, although the process completely occurred in the diffusion region [27]. The effective diffusion coefficient of water through a hydrated product layer depends on both the pressure of water vapor and the properties and history of the initial oxide film; it can vary by almost two orders of magnitude

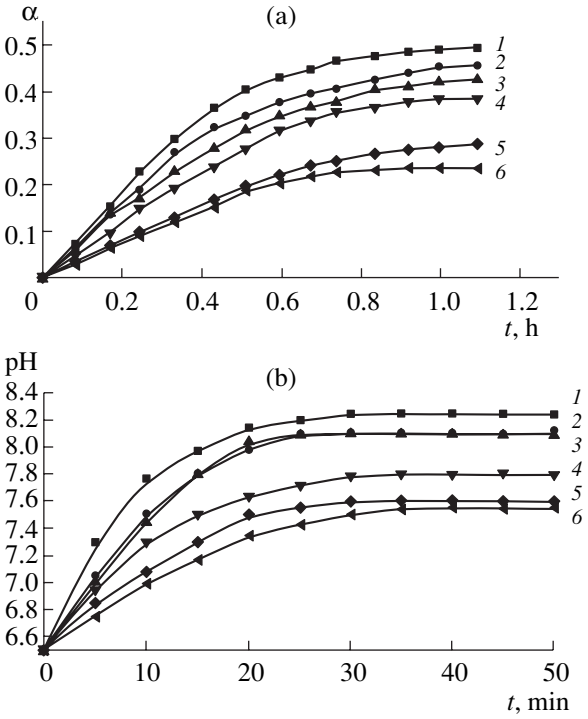

Fig. 6. (a) Kinetics of aluminum conversion (α) and (b) changes in the pH of solution in the course of hydrothermal oxidation at the following ratios between ASD-1 powder and water: (*1*) 1 : 20, (*2*) 1 : 100, (*3*) 1 : 200, (*4*) 1 : 300, (*5*) 1 : 400, and (*6*) 1 : 800.

[27]. Under the given conditions, it was found that the product underwent aging in the course of chemical oxidation reaction. This aging included the hydration and polymerization of anodically dissolved aluminum ions, phase transitions, and texture changes in the hydroxo compounds of aluminum; this noticeably affected the texture and phase composition of aluminum oxide obtained by thermal decomposition [28]. In particular, the true density of Al_2O_3 formed upon the calcination of composites increased from ~2.3 to ~3.5 g/cm^3 [10] as the temperature in the autoclave was increased. Moreover, the fraction of Al_2O_3 in cermets increased in the course of reaction; however, the specific surface area of alumina as a constituent of the composite decreased [28]. The rate of decrease in the specific surface area depended on the ratio between the rates of aluminum oxidation and aging of aluminum hydration products.

Table 2. Chemical reaction parameters of the hydrothermal oxidation of ASD-1 aluminum

Reference concentration of aluminum in water, g/l	1 : 20	1 : 100	1 : 200	1 : 300	1 : 400	1 : 800
w, l g^{-1} min^{-1}	0.0195	0.017	0.016	0.013	0.009	0.008
τ_{kin}, min	8	10	12	14	16	20
k, h^{-1}	1.22	1.13	0.9	0.71	0.7	0.69
n	1.01	1.034	1.08	1.2	1.51	1.55

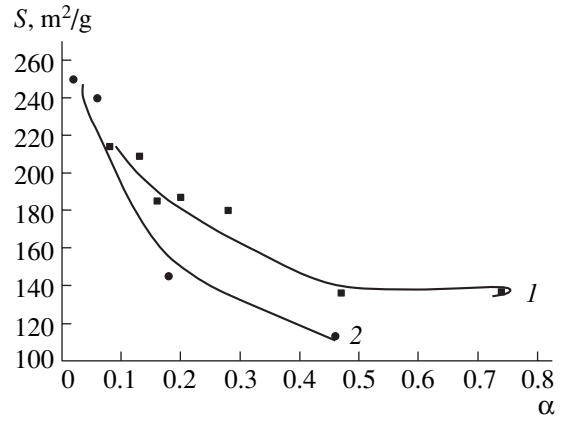

Fig. 7. Dependence of the specific surface area of aluminum oxide in the Al_2O_3/Al composite on aluminum conversion in hydrothermal oxidation for two types of PAHP aluminum powder particles (from [27]): d = (*1*) 50 or (*2*) 200 μm.

Thus, under almost constant external conditions, the rates of aging remained unchanged with the average particle size of aluminum, whereas the specific rate of oxidation decreased. This fact can explain a decreased specific surface area of alumina as a constituent of the Al_2O_3/Al composite obtained from a coarser fraction of aluminum at high conversions (Fig. 7) [28]. Analogous behaviors were also observed previously [27, 28].

In a number of cases, Al_2O_3 was obtained as a result of hydrothermal oxidation; the degree of hydration of the product increased as the distance from the surface of aluminum metal increased [30]. It is most likely that this phenomenon resulted from self-heating, which caused the rapid dehydration of hydrothermal oxidation products in the course of the rapid exothermic aluminum oxidation. As the distance from the reaction zone increased, the resulting amorphous oxide on the aluminum surface was hydrolyzed once again under hydrothermal conditions [31].

The reactivity of aluminum noticeably changed upon the encapsulation of powdered oxide additives under hydrothermal conditions. For these composites, the relationship between the composition and conversion was also more complicated. Thus, in the simplest case, for water-insoluble MO_x (without the carryover of substances from the die), the relationship between the conversion of aluminum and the additive content of the composite (z) is determined by the following equation [11]:

$$z = \frac{z'}{1 + \alpha X_0(1 - z')}, \qquad (9)$$

where z' is the weight fraction of the oxide additive in the initial mixture. As estimated using various oxide additives, alkaline-earth additives, as well as the Na forms of zeolites, which are favorable for loosening a product layer, increased α. Additives based on silicon dioxide or titanium dioxide, which forms a protective film on the surface of aluminum, noticeably decreased the conversion of aluminum [11, 33].

Oxide additives undergo noticeable changes under hydrothermal conditions. Most oxides undergo hydration [11]. Lanthanum hydroxide, which is usually stable on calcination in air at 700°C, underwent dehydration to form defect lanthanum oxide after hydrothermal treatment and calcination at 540°C [11]. However, hydrothermal treatment exerted the most significant effect on soluble oxide additives, because it facilitates the carryover of an oxide portion from the press mold to the autoclave, as was observed with CaO [11].

Based on the experimental results, we tested the inverse transfer method: the introduction of metal nitrates (5 mol %) into the Al_2O_3/Al composite from a solution in an autoclave with the simultaneous hydrothermal oxidation of aluminum at 200°C (2 h) followed by calcination. To evaluate the transfer of the oxide additive from the solution to the die, we used the molar transfer coefficient, which was determined through the mole fraction of MO_x (z''_μ) for the initial number of moles of aluminum (m^0_{Al}):

$$z''_\mu = \frac{n_{MO_x}}{n_{Al}} = \frac{m_{MO_x}}{\mu_{MO_x}}\frac{\mu_{Al}}{m^0_{Al}} = \frac{z''\mu_{Al}}{\mu_{MO_x}}, \qquad (10)$$

where n is the number of moles, and μ_{MO_x} and μ_{Al} are the molecular weights of the oxide and aluminum, respectively. The value of z'' is determined by the concentration of MO_x (z) in the MO_x/Al_2O_3/Al composite from the results of chemical analysis and the expected oxide stoichiometry based on X-ray diffraction data.

The molar transfer coefficient is equal to

$$z_\mu = \frac{\mu_{Al}}{\mu_{MO_x}}\frac{1 + \alpha X_0}{\frac{1}{z} - 1}. \qquad (11)$$

It was found that the molar transfer coefficient increased with decreasing cation mass (atomic number): Mg (4.2×10^{-2}) > Ca (2.2×10^{-2}) > La (0.9×10^{-2}). Only the coefficient of Ti (0.5×10^{-2}) drops out of this order; the salt of titanium was strongly hydrolyzed in the course of hydrothermal oxidation to form a white precipitate, which inevitably caused a considerable decrease in the concentration of titanium nitrate in solution. A physical reason for the relatively simple relationship in the majority of test oxides can consist in the diffusion of solutes across the surface of the parts of a die covered with a film of H_2O under conditions of an equilibrium pressure of water vapor. The total concentration of an oxide additive in the composite thus prepared varied from ~1 wt % for TiO_2 to 6 wt % for MgO. The conversion of aluminum in cermets with alkaline-earth and titanium oxides added increased by a factor of ~1.5, whereas the reactivity of aluminum remained unchanged after the addition of La_2O_3 (Table 1).

Organic additives usually decreased significantly the reactivity of aluminum [33]. Thus, at the stage of hydrothermal synthesis, the properties of cermets can be varied over a wide range.

5. THERMAL TREATMENT OF THE PRODUCTS OF HYDROTHERMAL SYNTHESIS

In general, two dramatically different regions of processes occurring upon the thermal treatment of the products of hydrothermal synthesis in air can be distinguished. At temperatures lower than the melting point of aluminum, exo and endo effects characteristic of the thermal decomposition of hydroxo compounds and metal salts were predominant. In some cases, exo effects appeared due to either the partial oxidation of aluminum metal upon the formation of cracks in oxide additives or the dehydration mechanism of oxides localized on the surface of aluminum metal in the course of synthesis under hydrothermal conditions [28]. Above the melting point of aluminum, the agglomeration of active alumina and the polymorphic transformation of active alumina into corundum occurred. The oxidation of aluminum with atmospheric oxygen occurred through the step of metal melting with the formation of a system of interconnected filamentary crystals of corundum [35]. It is of particular importance that the melting of aluminum in granulated composites with high concentrations of Al_2O_3 was not accompanied by their degradation. Thus, high-strength products of various shapes can be obtained. The formation of filamentary crystals (corundum whiskers) that reinforced the composite may be responsible for the enhanced strength [37].

As an example, the results of the differential thermal analysis (DTA) of the products of hydrothermal synthesis prepared from the solutions of Ca, La, Mg, and Ti nitrates by modification in an autoclave are given. Based on a comparison of experimental results with both published data [38–41] and the thermograms of individual salts (Ca, La) (Fig. 8), conclusions were drawn on processes occurring as the temperature was increased. The DTA curves of all of the samples show endotherms due to aluminum melting at ~650°C, as well as exotherms at 625–660°C and higher temperatures accompanied by weight gain due to the oxidation of aluminum metal; this is characteristic of all of the cermets based on aluminum (Fig. 8). The DTA curves of some samples (La, Ca, Ti) exhibits endothermic peaks accompanied by weight losses at 100–140 and 500–540°C. This DTA curve is characteristic of boehmite, which is usually formed in the oxidation of aluminum powder under these conditions (Fig. 8). For the Mg-containing composite, such a peak was shifted to lower temperatures (~400°C). Previously, Koryabkina and coauthors [40, 41] noted the same effect of a magnesium nitrate additive on the decomposition temperature of aluminum hydroxides. An analogous effect was also observed in mechanical mixtures of aluminum and magnesium hydroxides. Based on X-ray diffraction and spectroscopic data, the conclusion was drawn that no detectable interaction between hydroxo compounds occurred, although peaks in the DTA curves are shifted [40].

At the same time, endothermic peaks with relatively high weight losses, which are characteristic of nitrate compounds (except for titanium), appeared in a temperature range from 100 to 500°C: Ca, 145°C; La, 400°C; Mg, 170 and 370°C. It is likely that nitrates were partially retained in composite pores after hydrothermal treatment [39, 40]. For the Mg-containing composite, the endotherms at 250 and 300°C can be attributed to the decomposition of hydrargillite [38].

Thus, individual compounds of aluminum and additive elements were mainly formed in the thermal decomposition of hydrothermal oxidation products obtained in the presence of salt solutions. Taking into account that the calcination temperature was low, we believe that, in the majority of composites, oxide additives mainly occurred as individual oxides weakly interacting with the Al_2O_3/Al matrix. The exception is the Ca-containing composite, whose thermoanalytical curves are similar to the thermoanalytical curves of the double salt $Ca(AlO_2)_2 \cdot 3Ca(OH)_2 \cdot nH_2O$ [42]. It is likely that a solid solution based on calcium oxide or aluminate can be formed upon the thermal degradation of this compound. Upon the high-temperature treatment of hydrothermal synthesis products with a powdered alloy of nickel and chromium, its degradation with the formation of the intermetallic compounds of aluminum with nickel and chromium as a result of the interaction of Nichrome with molten aluminum was observed [43].

6. MAIN PROPERTIES OF COMPOSITES

6.1. Texture Properties

6.1.1. Total pore volume. Tikhov *et al.* [10] proposed the following equation to relate the specific pore volume (V_α) to the conversion and packed density of parent aluminum powder in a rigid die:

$$V_\alpha = \frac{1}{\delta_0(\alpha X_0 + 1)} - \frac{1-\alpha}{\rho_{Al}(\alpha X_0 + 1)} - \frac{\alpha(X_0 + 1)}{\rho_{Al_2O_3}(\alpha X_0 + 1)}. \quad (12)$$

In Eq. (12), the packed density (δ_0) and the true densities of aluminum (ρ_{Al}) and Al_2O_3 ($\rho_{Al_2O_3}$) were determined independently for each powder and cermet (X_0 is the relative weight change). In a number of cases, the averaged true densities of Al_2O_3 were used with consideration for the dependence of the density on the conditions of hydrothermal oxidation [10]. The value of α for various aluminum powders depending on the reaction

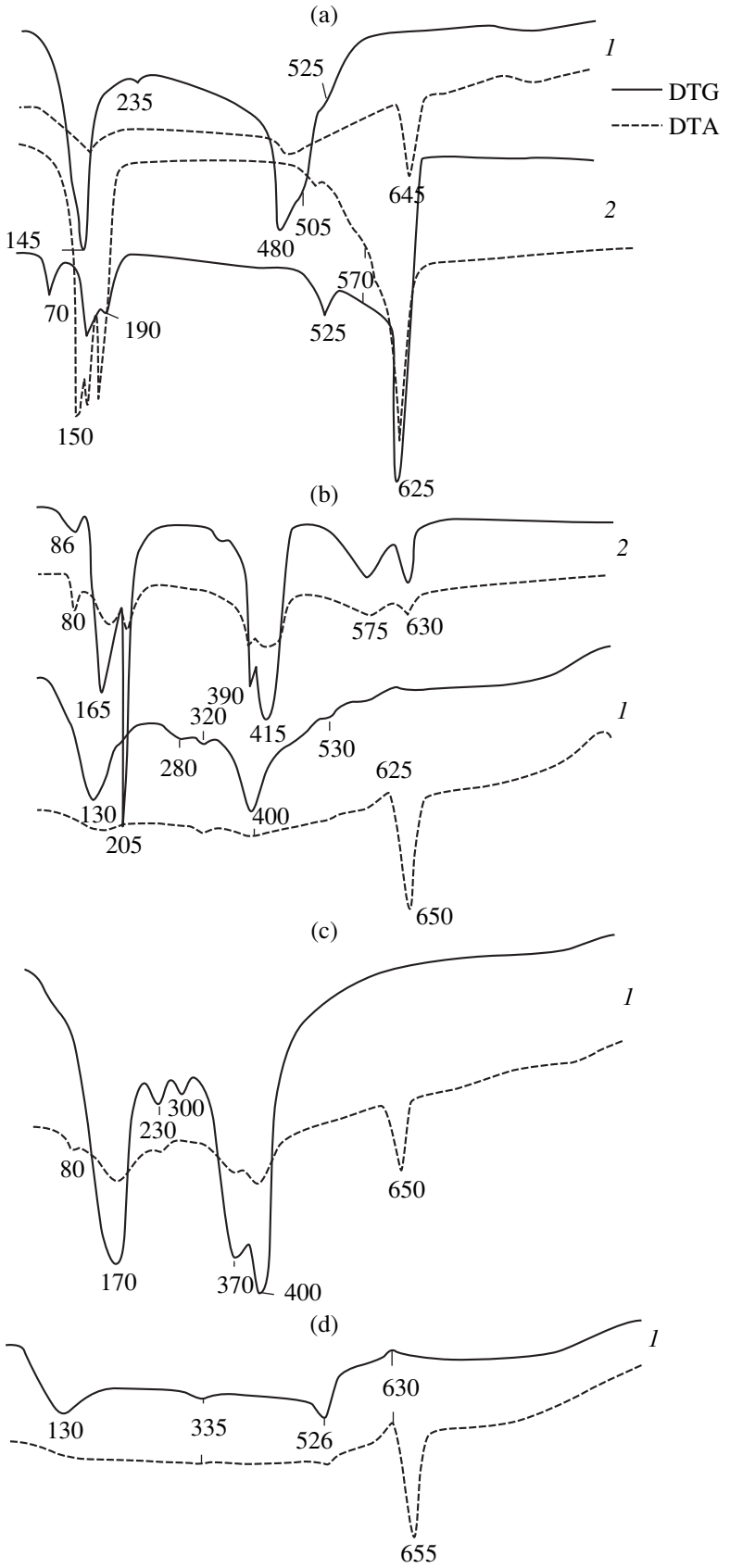

Fig. 8. Thermoanalytical curves for (*1*) hydrothermal synthesis products (200°C; 2 h) prepared by the hydrothermal oxidation of PA-4 aluminum in an autoclave containing the solutions of (a) Ca, (b) La, (c) Mg, and (d) Ti nitrates. For comparison, the curves for (*2*) pure salts are given. Peak temperatures in °C.

conditions of oxidation can be predicted taking into account available rate laws (see Eq. (8) and [11]).

Equation (12) is applicable when the properties of composite components are additive in the absence of substance carryover from the die and a noticeable shrinkage of granules. Moreover, oxidation should not occur at the step of thermal treatment in air (although this can also be taken into consideration with the use of corresponding true densities for high-temperature modifications of alumina).

Figure 9 shows a graph that reflects the relationship between the experimental pore volume (found from the true and apparent densities of pellets [10]) and the pore volume calculated using analytic expression (12). The experimental results and calculated data were consistent over wide ranges of cermet compositions, aluminum conversions, and hydrothermal oxidation reaction conditions. Somewhat underestimated calculated values, as compared with experimental data, were usually observed at great values of α. Under these conditions, aluminum hydroxide was formed, which was converted into Al_2O_3 after calcination. In this case, the shrinkage of cermet granules was possible. This shrinkage was insignificant for pellets with characteristic sizes of 5–10 mm; however, we observed it in large monoliths of ~50 mm. The shrinkage (and, consequently, the accuracy of predictions for the total pore volume) can be evaluated quantitatively with the use of a shrinkage factor (f_v). We determined this shrinkage factor from the ratio of the composite granule volume after calcination to the volume of the press mold [10].

For the $MO_x/Al_2O_3/Al$ composites prepared by encapsulation, the total pore volume was calculated from the following equation [12]:

$$V_\alpha = \frac{1}{\delta_0[1+\alpha X_0(1-z')]} - \frac{(1-\alpha)(1-z')}{\rho_{Al}[1+\alpha X_0(1-z')]} - \frac{\alpha(X_0+1)(1-z')}{\rho_{Al_2O_3}[1+\alpha X_0(1-z')]} - \frac{z'}{\rho_{MO_x}[1+\alpha X_0(1-z')]}. \quad (13)$$

As calculated from Eq. (13), the first three terms of the equation make the main contribution to the total pore volume [11]. This equation is valid in the absence of considerable shrinkage (characteristic of composites prepared with the use of oxide additives with developed internal surfaces, such as MgO and Al_2O_3) or when the carryover of oxides from the volume of the die is insignificant. If the carryover occurs (as in the case of CaO), the following equation can be used [11]:

$$V_\alpha^* = \frac{f_v(1-z)}{\delta_0(1-z')(1+\alpha X_0)} - \frac{(1-\alpha)(1-z')}{\rho_{Al}[1+\alpha X_0(1-z')]} - \frac{\alpha(X_0+1)(1-z)}{\rho_{Al_2O_3}(1+\alpha X_0)} - \frac{z'}{\rho_{MO_x}[1+\alpha X_0(1-z')]}. \quad (14)$$

Equation (14) was obtained on the assumption that calcium oxide and alumina occur individually in the composite without the formation of aluminum–calcium spinel. Taking into account that the contribution of the last term of the equation is small, this assumption does not significantly affect the total pore volume.

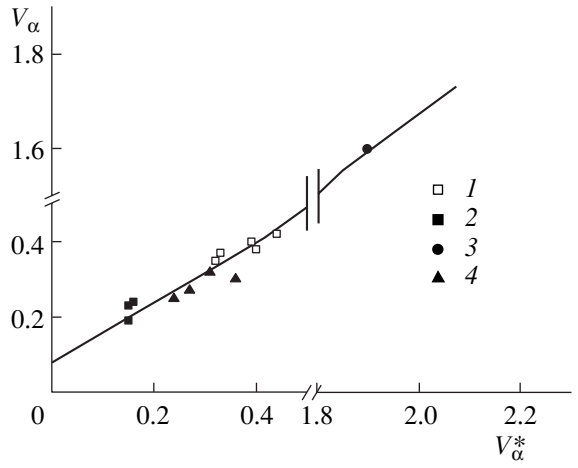

Fig. 9. Relationship between pore volumes calculated from Eq. (12) (V_α) and evaluated from experimental data (V_α^*): (*1*) PA-4 (hydrothermal oxidation at 150–250°C), (*2*) PAHP (hydrothermal oxidation at 150–250°C), (*3*) silver-like aluminum powder (hydrothermal oxidation at 100°C), and (*4*) PAHP (hydrothermal oxidation at 120°C, organic alcohols).

The substance can be transferred not only from the press mold to the solution in the autoclave but also vice versa. Using this phenomenon, we synthesized a number of composites from soluble metal salts. The amount of an additive introduced into the Al_2O_3/Al composite was evaluated from chemical analysis data. It should be taken into account that aluminum oxide and aluminum metal are separated by a clear interface, whereas this is not evident in the general case of MO_x and Al_2O_3. In particular, as demonstrated above, mixed calcium and aluminum hydroxo compounds were formed upon hydrothermal oxidation. It is most likely that they were retained as mixed oxides upon thermal decomposition. Unfortunately, the true density of these mixed oxides cannot be determined accurately. Therefore, as a first approximation, we assumed that it is proportional to the fraction of corresponding simple oxides. Thus, we derived the following equation for evaluating the specific pore volume in the case of substance transfer from the autoclave to the die:

$$V_\alpha^* = \frac{1}{\delta_0(1+\alpha_R X_0+z'')} - \frac{1-\alpha_R}{\rho_{Al}(1+\alpha_R X_0+z'')} - \frac{\alpha_R(1+X_0)}{\rho_{Al_2O_3}(1+\alpha_R X_0+z'')} - \frac{z''}{\rho_{MO_x}(1+\alpha_R X_0+z'')}. \quad (15)$$

In Eq. (15), the true densities of oxides were taken from handbooks [12, 13]. The density of Al_2O_3 was determined as described above.

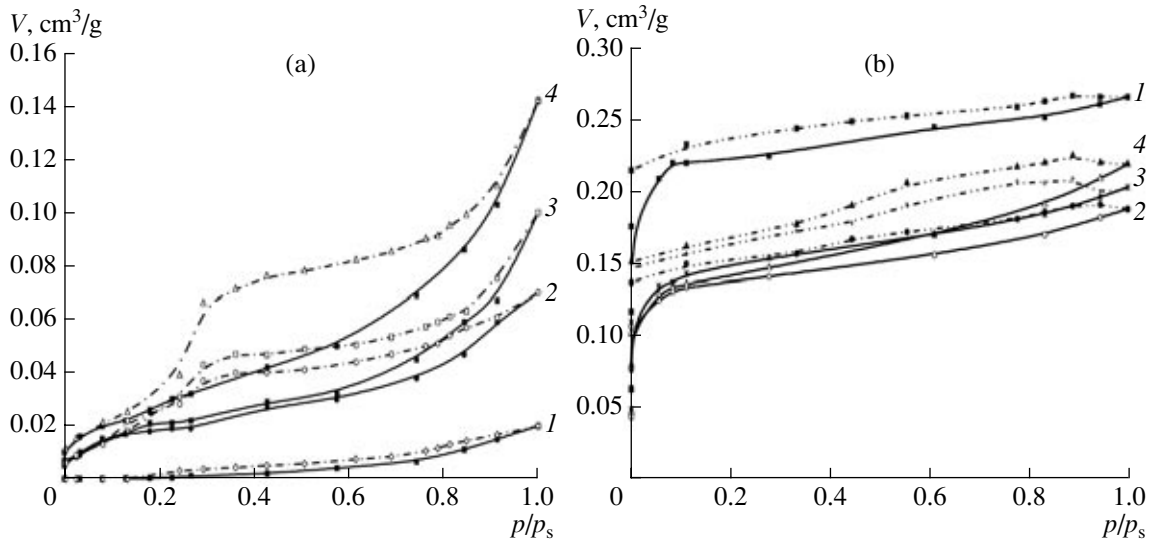

Fig. 10. Sorption isotherms of (a) benzene and (b) water on (*1*) NaA zeolite and the synthesized NaA/Al_2O_3/Al composite at a 2 : 1 ratio (by weight) between initial powder components and zeolite particle sizes of (*2*) 0.5–1.0, (*3*) 0.3–0.5, and (*4*) 0.1–0.3 mm. Solid and dashed lines refer to adsorption and desorption, respectively (ASD-1 aluminum powder).

The resulting expressions can be used for predicting pore volumes in the syntheses of cermets with oxide additives. Data given in Table 1 indicate that the introduction of additives from solution significantly decreased the pore volume of the composite. This is a difference from the MO_x/Al_2O_3/Al complex composites synthesized by powder mixing, whose pore volume increased upon the introduction of additives [11]. It is likely that the procedure of introducing an additive from solution under hydrothermal conditions is similar to the procedure of impregnating granular supports (on supporting an active component or modifier), although granulation and the introduction of an oxide additive are combined in a single stage in the former case.

6.1.2. Micropore and mesopore structures of composites. In the range of pore sizes up to 100 nm, the Al_2O_3/Al simple composites exhibited a narrow pore-size distribution with a maximum at 3–10 nm depending on the conditions of hydrothermal synthesis (with the determination of porosity using a standard method [28, 44]). The pore structure of MO_x/Al_2O_3/Al prepared by encapsulation can be either similar to the pore system of Al_2O_3/Al composites (if the porosity of MO_x is low) or significantly different because of the porosity of oxide additives. Oxide additives can also affect the porosity by changes in the reactivity of aluminum. Since individual components vary in porosity, the adsorption properties of composites can be widely varied. Thus, on the encapsulation of NaA zeolite, whose channel size is 0.4 nm, the adsorption isotherms of benzene and water were significantly different (Fig. 10). The pores of NaA zeolite are inaccessible to benzene molecules with a kinetic diameter of ~0.6 nm; therefore, the adsorption isotherms were comparable in shape to the adsorption isotherms of nitrogen on Al_2O_3/Al. In this case, the fraction of alumina and the adsorption volume increased as the particle size of oxide additives was decreased (Fig. 10a). At the same time, the shape of the adsorption isotherms of water vapor remained close to the isotherms for pure zeolite, and the dependence on the particle size of oxide additives became noticeably weaker. The pore volume as an extremal function of the aluminum content of the starting mixture (Fig. 11) can also be explained by the effect of zeolite on the reactivity of aluminum (and on the concentration of aluminum oxide).

For a composite containing NaY zeolite with pores of ~0.7 nm, the sorption pore volume and the dependence of the adsorption isotherms of benzene and water on the fractional makeup of the zeolite differed only slightly (Fig. 12).

The adsorption isotherms of nitrogen on MO_x/Al_2O_3/Al composites prepared by modification from solution in an autoclave are closer to the type H3 of the shape of a hysteresis loop in terms of the IUPAC classification (Fig. 13). The type H2 adsorption isotherms on a sample of the Al_2O_3/Al composite are characteristic of a three-dimensional micropore structure with a mutually intersecting pore network (see [28] and Fig. 13). Thus, the additives introduced from solution facilitate the formation of a less ordered texture of the oxide components of cermets. The pore structure was described in detail based on a comparative analysis of the shapes of adsorption–desorption curves [45]. From Table 3, it follows that, except the Ca-containing composite, the total specific surface area and the outer surface of aggregates increased in all of the samples. A change in the macrorelief, as compared with the parent Al_2O_3/Al composite, is also evident from scanning electron microscopy (SEM) data (Fig. 14). In particu-

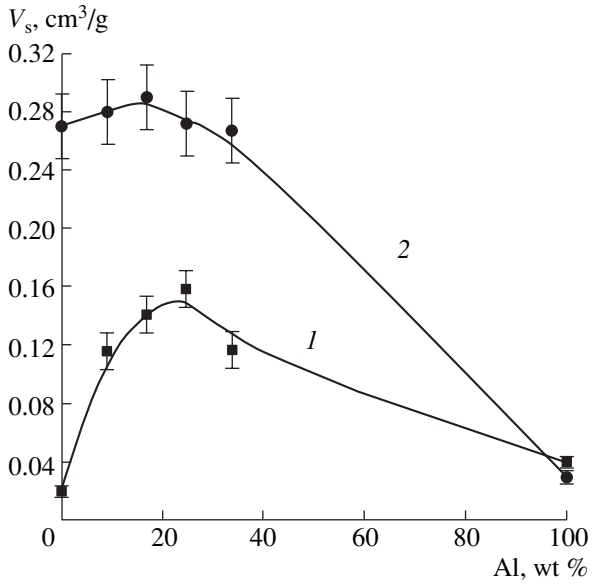

Fig. 11. Dependence of the pore volume of the NaA/Al_2O_3/Al composite on the concentration of aluminum upon the sorption of (*1*) benzene and (*2*) water vapor (ASD-1 aluminum powder).

lar, the shapes and sizes of aggregates were similar in the Mg- and La-containing composites prepared from solutions and powders [11]. The specific surface area of the oxide component is somewhat larger in La- and Ti-containing composites. Taking into account that oxide additives affect both of the characteristics, we can conclude that additives like CaO, which interact with aluminum hydroxides, are favorable for decreasing the average sizes of both primary particles and oxide aggregates in the composite. The former can be explained by the formation of MO_x particles smaller than Al_2O_3 particles. The latter is likely due to changes in the aggregation processes of primary aluminum hydroxide particles because the fraction of MO_x in the total concentration of the oxide additive is small.

The specific volume of pores with sizes up to 100 nm, as determined from adsorption data, and the average pore size changed insignificantly (except for the Ca-containing cermet) (Table 3). It is likely that the formation of primary aluminum hydroxide (oxide) particles occurred more rapidly than the diffusion of dissolved additives into the die, and the additives were mainly concentrated at the outer surface of aggregates. The formation of calcium aluminate was favorable for a considerable decrease in both the specific surface area and the pore volume [17].

6.1.3. Ultramacropores. We compared the pore volumes evaluated from the true and apparent densities of cermets with the values obtained from mercury porosimetry data and found that the latter were considerably smaller (by a factor of 2–4). This fact can most likely be explained by the presence of ultramacropores with sizes greater than 10 μm, which were spontaneously filled at a minimum pressure of mercury [10]. These pores cannot be detected by mercury porosimetry. This cannot be explained by the amalgamation of aluminum by mercury because, if this were the case, the experimental values of the pore volume would be overestimated, as compared with the calculated values of the apparent and true densities of the composites. For the parent aluminum powder with a minimum thickness of the oxide film, mercury porosimetry data were only 25–30% lower than the calculated values based on the true and apparent densities of granulated aluminum. Analogously, the difference between mercury porosimetry data and estimated values based on densities was no greater than 20% for granular supports of A-1 Al_2O_3. Pores of size > 50 μm were detected using SEM (Fig. 5). The crucial factor affecting the macropore structure is the packed density of the starting powder mixture (see Section 2).

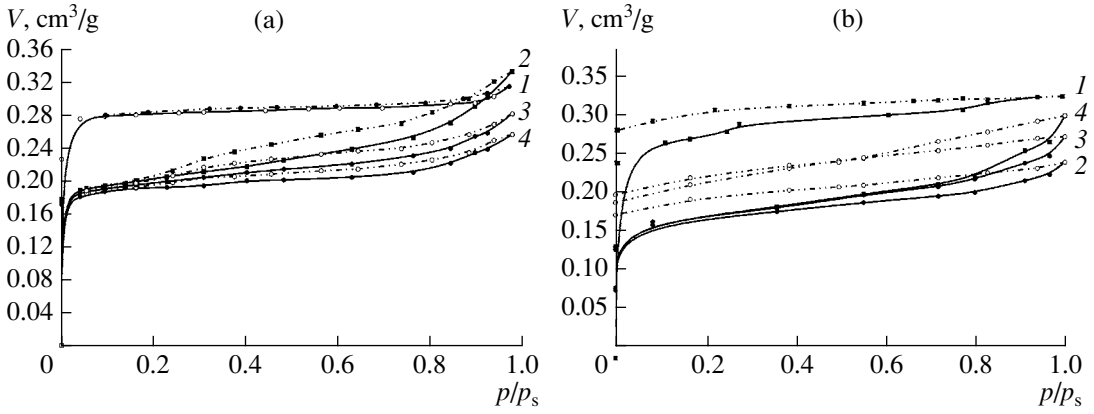

Fig. 12. Sorption isotherms of (a) benzene vapor and (b) water vapor on (*1*) NaY zeolite and the synthesized NaY/Al/$Al(OH)_3$ composite at a 3 : 1 weight ratio between components with zeolite particle sizes of (*2*) 0.5–1.0, (*3*) 0.3–0.5, and (*4*) 0.1–0.3 mm. (ASD-1 aluminum powder).

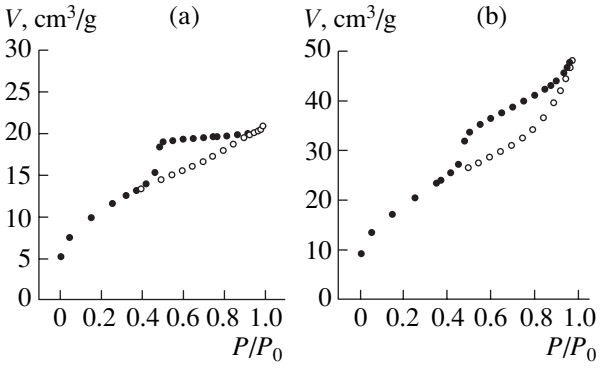

Fig. 13. Typical isotherms of nitrogen adsorption for (a) Al_2O_3/Al and (b) MO_x/Al_2O_3/Al composites prepared by modification with metal nitrates (5 mol %) (M = Ca, La, Mg, or Ti). Conditions of hydrothermal synthesis: 200°C; 2 MPa; 2 h (PA-4 aluminum powder).

The presence of ultramicropores is responsible for the high diffusion permeability of granular cermets. Although this permeability is lower than the permeability of foam materials, it is much higher than that of traditional porous oxide ceramics and is equal to $2.8–6.6 \times 10^{-13}$ m^2 [32]. Because of these properties, porous cermets are promising for use as filter elements and supports for membranes and catalysts.

6.1.4. Common features of the texture of cermets based on Al_2O_3/Al. A comparison of data obtained by mercury porosimetry, adsorption methods, and calculations based on the apparent and true densities allowed us to represent the texture properties of composites based on Al_2O_3/Al in a generalized form (Fig. 15).

All of the test porous composites prepared by the oxidation of aluminum powder under hydrothermal conditions were characterized by a hierarchical polydisperse pore structure. Based on texture properties, these cermets can be assigned to a class of materials intermediate between traditional high-porosity oxide ceramics and foam materials [46]. Micropores and mesopores in these materials can be controlled by both the conditions of hydrothermal synthesis and the modification of composites. In this case, the fraction of these pores in cermets increases as the fraction of microporous oxide ceramics is increased. The macropore structure essentially depends on the particle-size distribution of the initial mixture, although the proportions of micropores and macropores changes depending on the conversion of aluminum in rigid press molds. The presence of a developed network of ultramacropores is responsible for the high diffusion permeability of these cermets.

6.2. Factors Determining Mechanical Properties

The formation of mechanically strong monoliths in the hydrothermal oxidation of aluminum can be characterized by the following main features:

• Mechanically strong catalysts are formed even before the stage of calcination in air, that is, even in the course of hydrothermal synthesis.

• The cementation of aluminum particles to form a solid monolith occurs simultaneously with the reaction of hydrothermal oxidation at the stage of diffusion inhibition, when the reagent is covered with a layer of aluminum hydroxo compounds [27].

• The hydrothermal oxidation reaction is accompanied by the transfer of hydrothermal oxidation products to the sites of contacts between aluminum particles by either oriented growth [47] or dissolution in an alkaline medium followed by transfer to sites with a smaller radius of curvature [48].

• The "reagent" concentration for catalyst formation is determined by the reaction of hydrothermal oxidation and its special features.

Table 3. Texture characteristics of MO_x/Al_2O_3/Al composites prepared from solutions (PA-4 aluminum powder)

MO_x	Composition, fraction		Pore volume, cm^3/g			Specific surface area, m^2/g			Pore size, nm
	z	y'	V_μ	V_{aggr}	V_{outer}	S_Σ	S_{outer}	S_{ox}	
–	–	0.19	0.001	0.026	0.14	31.5	2.9	166	1.9
CaO	0.04	0.22	0.001	0.025	0.06	20.6	6.1	79	2.2
La_2O_3	0.05	0.18	0.005	0.024	0.11	51.5	15.5	224	1.4
MgO	0.06	0.25	0.001	0.024	0.08	48.0	15.4	155	1.6
TiO_2	0.01	0.24	0.001	0.031	0.11	49.7	17.2	199	1.8

Notes: z and y' are specified in Table 1.
V_μ is the specific ultramicropore volume.
V_{aggr} is the specific micropore and mesopore volume within aggregates.
V_{ox} is the specific pore volume within aggregates referenced to the oxide component of the cermet ($V_{ox} = (V_\mu + V_{aggr})/(x + y')$).
S_Σ is the specific surface area of the cermet.
S_{outer} is the outer surface area of aggregates.
S_{ox} is the specific surface area of the oxide component of the cermet.

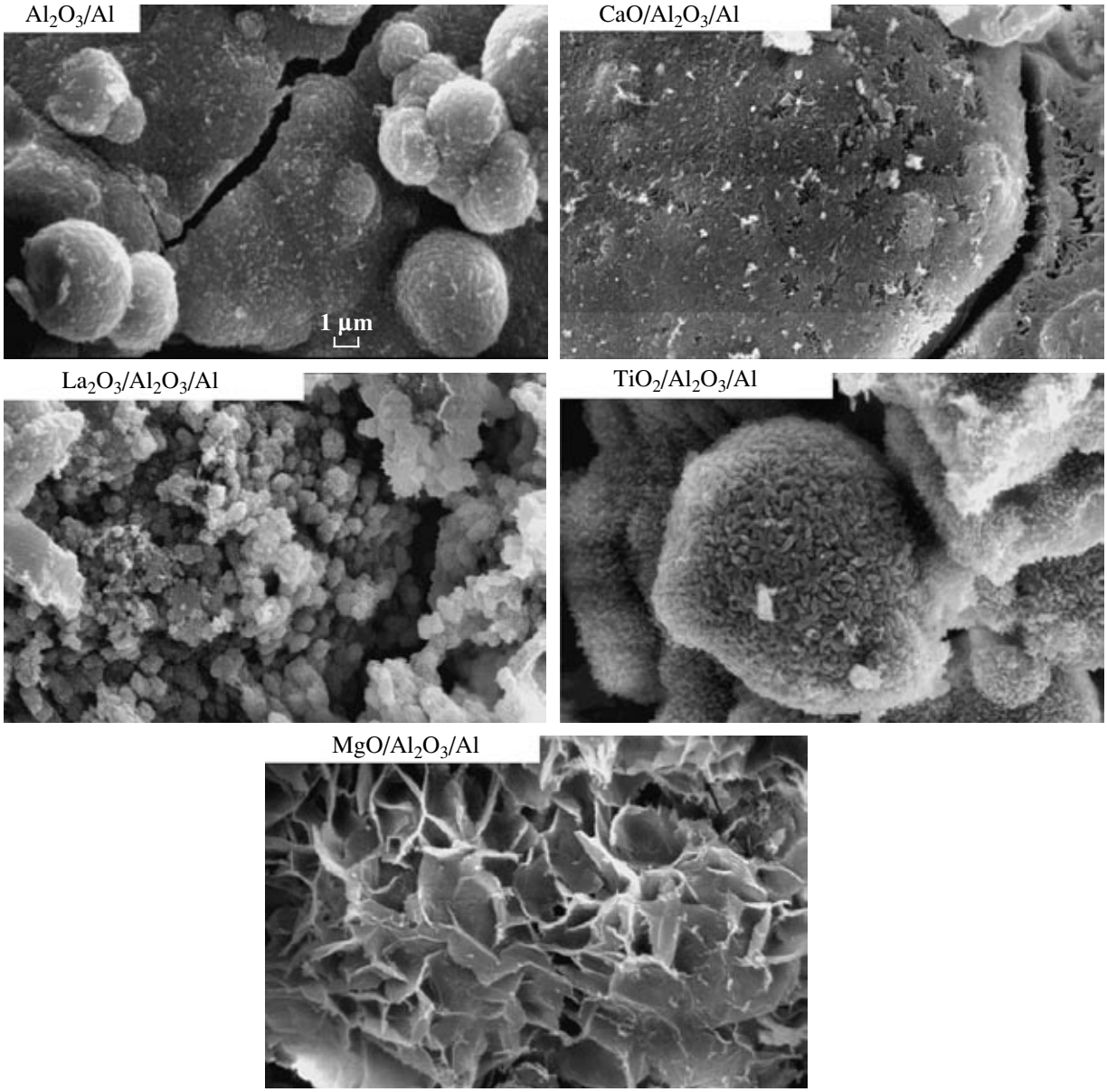

Fig. 14. Electron micrographs of composites prepared by modification from an autoclave solution.

• An increase in the volume of a solid in a rigid press mold at high conversions is of importance; this increase results in the self-pressing of composite particles to form a solid monolith [10].

As a rule, the introduction of oxide additives into a mixture with aluminum significantly decreased the strength of monolith composites [11]. The strength of these composites increased with aluminum conversion [32], although the chemical properties of oxide additives undoubtedly changed because of the surface decoration of oxide particles with hydrothermal oxidation products. To determine the dependence of the mechanical strength of synthesized composites on the particle sizes of zeolite and Al_2O_3 powders and on the concentrations (weight fractions) of these powders mixed with ASD-1 aluminum, we constructed a standard orthogonal design matrix for an all-factor experiment [49–52] (Fig. 16). The adsorbent particle size and weight fraction were varied over the ranges 0.2–0.8 μm and 0.70–0.89, respectively. The experimental design matrix and data processing allowed us to obtain an approximation model for the dependence of mechanical strength on adsorbent particle size and weight fraction in the mixture as the following regression equations in code variables for the A-1 aluminum oxide/Al_2O_3/Al and NaA zeolite/Al_2O_3/Al porous composites, respectively:

$$\Pi = 162.59 + 156.64r - 122.83z - 232.9rz, \quad (16)$$

$$\Pi = 295.18 - 325.52r - 285.76z + 321.53rz. \quad (17)$$

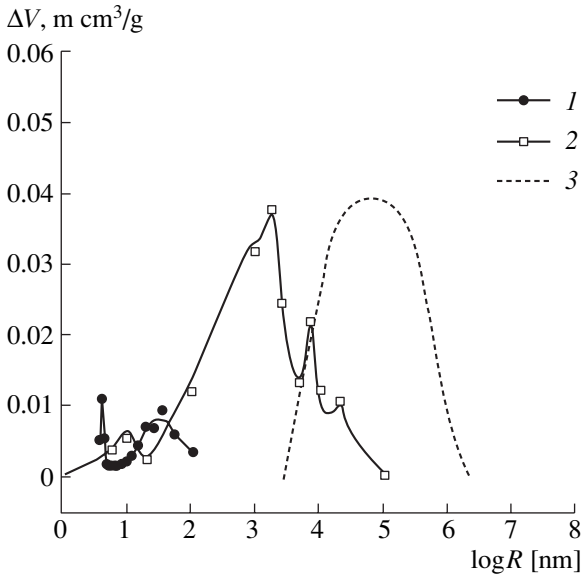

Fig. 15. Typical pore-size distributions (ΔV is the pore volume increment) for cermet composites according to data obtained by various techniques: (*1*) adsorption–desorption isotherms of N_2, (*2*) mercury porosimetry, and (*3*) pore volume evaluated from the difference between the specific volume and volume according to mercury porosimetry data and N_2 isotherms.

These equations reflect the dependence of the mechanical strength (Π) of samples on the particle size (r) and weight fraction (z) of a powdered adsorbent. The deviation between calculated and experimental data falls in the range 0.05–0.07, which indicates that the values of Π can be calculated at given values of r and z. The reproducibility of the results was evaluated using the Cochran test at equal numbers of simultaneous experiments at each combination of the levels of factors. In this case, the reproducibility variance was $S_y^2 = 1.85$ or 9.08 for the A-1/Al_2O_3/Al or NaY/Al_2O_3/Al samples, respectively. The experimental relationships (Fig. 16) reflect a general tendency in changes in the mechanical properties of pellets depending on the composition and size of a coarse fraction (as compared with aluminum powder) of oxide additives: a decrease in the strength with increasing particle size and concentration of the additive, all other factors being equal. The mechanical strength of the porous A-1/Al_2O_3/Al composite was, on the average, 20–25% lower than the strength of the NaY/Al_2O_3/Al composite. This is likely due to the effect of Na^+ cations (through the generation of hydroxyl ions and a higher pH value than that for pure aluminum powder) on the dissolution of aluminum and the formation of interparticle contacts. In general, in spite of the developed macropore structure, composites obtained by the hydrothermal oxidation of aluminum powder exhibited a much higher mechanical strength, as compared with monoliths prepared by extrusion or nodulization.

6.3. Catalysts Based on Porous Cermets

Catalysts based on cobalt oxide, which were prepared by the encapsulation of basic cobalt carbonate, for the complete oxidation of hydrocarbons and CO were found to be most active among platinum-free catalysts. Analogous catalysts prepared by cementing

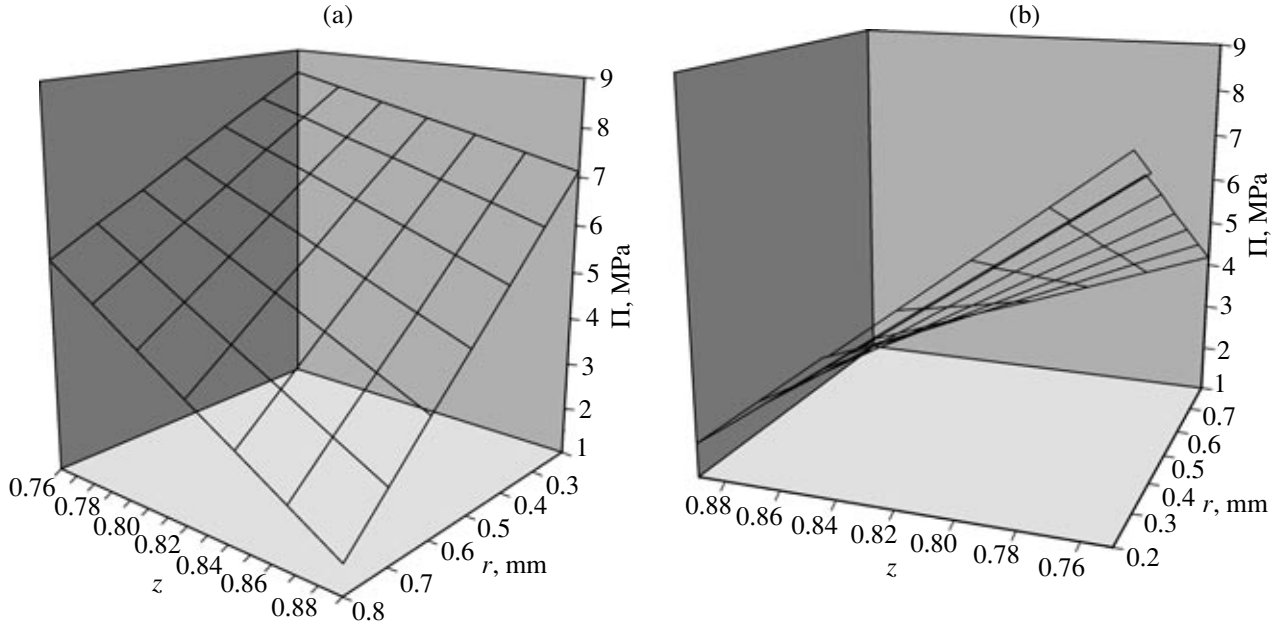

Fig. 16. Dependence of the mechanical strength (Π) of porous (a) NaY/Al_2O_3/Al and (b) A-1/Al_2O_3/Al composites on dispersity (r) and concentration of oxide additives (z) (ASD-1 aluminum powder).

show comparable activities, but they have a much lower mechanical strength [35].

Catalysts for methane steam reforming were prepared by the following two methods: (1) the introduction of basic nickel carbonate [53], nickel lanthanide [54], or an alloy of nickel and chromium [55]; (2) the encapsulation of mixed zirconium and alkaline-earth oxides followed by impregnation with a solution containing ruthenium [35]. As compared with Ni–Cr ceramic foam catalysts (granule size of 5–8 mm; 0.8 wt % Ni/CeO_2 + Ni–Cr/δ-Al_2O_3), which were proposed previously [56], the La–Ni-containing cermets with the addition of Nichrome powder (granule size of ~2 mm; 50 wt % Ni) prepared in this work exhibited a higher catalytic activity in the reaction of methane steam reforming (cf. 2.2 cm^3 CH_4 (ml Cat)$^{-1}$ s^{-1} bar^{-1} at 750°C, 50% methane conversion, and reaction mixture space velocity of 7100 h^{-1} and 3.5 cm^3 CH_4 (ml Cat)$^{-1}$ s^{-1} bar^{-1} at 750°C, respectively). After the introduction of an additional amount of nickel into the La–Ni-containing cermets by the impregnation method, the rate constant increased twofold under the same experimental conditions at a methane conversion of 78%. Thus, although the use of nickel is more effective in the case of foam materials, the activity of composite materials per unit volume is higher, and this is of practical importance. The developed macropore structure considerably weakens the dependence of activity on composite granule size, as compared with traditional catalysts such as GIAP-16 [54].

Systems prepared by the encapsulation of fused iron–potassium or iron–zirconium catalysts [57] were found to be active in the Fischer–Tropsch synthesis. Intermetallide hydrides were partially oxidized upon encapsulation; however, the active hydride phase was recovered after the interaction with a reaction atmosphere. Thus, comparatively mild conditions of encapsulation provide an opportunity to obtain granular materials capable of accumulating hydrogen.

Honeycomb substrates up to 50 mm in diameter for the catalysts of partial methane oxidation to synthesis gas were synthesized by the hydrothermal oxidation of aluminum powder in a mixture with cerium dioxide and Nichrome followed by high-temperature treatment in air. The resulting substrates were characterized by a sufficiently high microporosity, which allowed us to introduce an active component based on platinum and nickel by impregnation from solution [43] without supporting a porous substrate. They were also characterized by a high thermal-shock resistance and a high resistance to thermal gradients across the catalyst bed.

Note that the enhanced thermal conductivity of composite systems can be due to not only the encapsulation of metal powders or unoxidized aluminum (as compared with traditional porous ceramic supports, the thermal conductivity increased by a factor of 4–10 [32, 58]) but also self-fixation on an inner or outer surface of metal tubes (Fig. 17).

Fig. 17. Samples of composite coatings on the inner and outer surfaces of metal tubes.

CONCLUSIONS

The development of promising methods for the synthesis of new materials depends on the simplicity, manufacturability, flexibility, and possibility of using inexpensive and readily available raw materials. From this standpoint, the above method for the synthesis of porous metal ceramic and ceramic products is very promising. The results of this work allowed us to conclude that the new class of inorganic compounds, porous metal oxide materials prepared from aluminum powders by hydrothermal synthesis, can be of considerable interest for the manufacture of adsorbents, catalysts, filtering material, membrane supports, etc.

Various types of powdered, sparingly soluble raw materials that are stable under hydrothermal conditions (oxides, metals, hydrides, salts, etc.), as well as soluble compounds, can be used for the production of pelletized composite materials through the stage of hydrothermal synthesis. The composition and properties of cermet and ceramic composite materials can be varied over very wide ranges by varying synthetic procedures and starting raw materials, and hydrogen (which is an environmentally friendly fuel) is released in the course of production. In this case, 1.22 l of hydrogen is formed per gram of aluminum converted.

The materials synthesized by the given method cannot be prepared by any currently available method for the formation of porous solids. With respect to mechanical and thermophysical properties and pore structure, these cermets occupy an intermediate position between permeable porous materials prepared by the sintering of metal powders and ordinary highly porous oxide ceramics.

A disadvantage of the method for the synthesis of the above materials is that aluminum metal is rather expensive. Therefore, the use of aluminum metal can be economically sound with a considerable gain in the activity and selectivity of processes with the use of composite catalysts. The occurrence of unoxidized aluminum in cermets decreases their stability in atmo-

spheres containing water vapor. However, based on the above studies, methods can be developed for the almost complete oxidation of aluminum. Hydrogen, which is a by-product of the synthesis, is dangerously explosive; however, it can be used for practical purposes upon the development of adequate trapping systems. In any event, a final decision on the advantages and disadvantages of hydrothermal oxidation can be made on passing from laboratory-scale to pilot studies.

ACKNOWLEDGMENTS

We are grateful to Yu.V. Potapova and Yu.N. Dyatlova for the synthesis of samples, to A.N. Salanov who performed electron-microscopic studies, and to G.S. Litvak who performed thermal analysis.

REFERENCES

1. Andreeva, V.A., *Osnovy fiziko-khimii i tekhnologii kompozitov* (Composites: Fundamentals of Physical Chemistry and Technology), Moscow: IRZhR, 2001.
2. Sungkono, I., Kameyama, H., and Koya, T., *Appl. Surf. Sci.*, 1997, vol. 121/122, p. 425.
3. Patermarakis, G. and Nicopoulos, N., *J. Catal.*, 1999, vol. 187, p. 311.
4. Burgos, N., Paulis, M., Antxustegi, M.M., *et al.*, *Appl. Catal.*, vol. 38, p. 251.
5. Varghese, O.K., Gong, D., Paulose, M., *et al.*, *J. Mater. Res.*, 2002, vol. 17, no. 5, p. 1162.
6. Solntsev, K.A., Shustorovich, E.M., Chernyavskii, A.S., *et al.*, *Dokl. Akad. Nauk*, 2002, vol. 385, no. 3, p. 372.
7. Anan'in, V.N., Belyaev, V.V., Parmon, V.N., *et al.*, *Tezisy dokladov XIV Mendeleevskogo s"ezda po obshchei i prikladnoi khimii* (Proc. XIV Mendeleev Cong. on General and Applied Chemistry), Minsk: Navuka i Tekhnika, 1993.
8. Yakerson, V.I., Dykh, Zh.L., Subbotin, A.N., *et al.*, *Kinet. Katal.*, 1995, vol. 356, no. 6, p. 918.
9. *Poristye pronitsaemye materialy* (Porous Permeable Materials) Belov, S.V., Ed., Moscow: Metallurgiya, 1987, p. 175.
10. Tikhov, S.F., Fenelonov, V.B., Sadykov, V.A., *et al.*, *Kinet. Katal.*, 2000, vol. 41, no. 6, p. 907.
11. Tikhov, S.F., Potapova, Yu.V., Fenelonov, V.B., *et al.*, *Kinet. Katal.*, 2004, vol. 45, no. 4, p. 642.
12. Rabinovich, V.A. and Khavin, Z.Ya., *Kratkii khimicheskii spravochnik* (Concise Handbook of Chemistry), Leningrad: Khimiya, 1978.
13. *Spravochnik khimika* (Chemist's Handbook), Leningrad: Khimiya, 1968, vol. 2.
14. Fenelonov, V.B., *Kinet. Katal.*, 1994, vol. 35, no. 5, p. 795.
15. Fenelonov, V.B., *Extended Abstract of Doctoral (Chem.) Dissertation*, Novosibirsk: Inst. of Catalysis, 1987.
16. Peronius, N. and Sweeting, T.J., *Powder Technol.*, 1985, vol. 42, p. 113.
17. Shkrabina, R.A., *Extended Abstract of Doctoral (Chem.) Dissertation*, Novosibirsk: Inst. of Catalysis, 1997.
18. Riekert, L. and Ulrich, R., *Chem.–Ing.–Tech.*, 1984, vol. 56, no. 2, p. 149.
19. Zhilinskii, V.V. and Lokenbakh, A.K., *Latv. PSR Zinat. Akad. Vestis. Kim. Ser.*, 1988, no. 5, p. 622.
20. Zhilinskii, V.V., Lokenbakh, A.K., and Lepin, L.K., *Latv. PSR Zinat. Akad. Vestis. Kim. Ser.*, 1986, no. 2, p. 151.
21. Zhilinskii, V.V., Shcherbakov, V.K., Lokenbakh, A.K., *et al.*, in *Sovershenstvovanie protsessov lit'ya i obrabotki alyuminiya i proizvodstva kremniya* (Improvement of Aluminum Casting and Machining and Silicon Manufacture Processes), Leningrad: VAMI, 1985, p. 45.
22. Rat'ko, A.I., Romanenkov, V.E., and Krupen'kina, Zh.V., *Dokl. Nats. Akad. Nauk Belarusi*, 2003, vol. 47, no. 4, p. 55.
23. Rat'ko, A.I., Romanenkov, V.E., Bolotnikova, E.V., *et al.*, *Dokl. Nats. Akad. Nauk Belarusi*, 2003, vol. 47, no. 5, p. 62.
24. Erofeev, B.V., *Dokl. Akad. Nauk SSSR*, 1946, vol. 52, no. 6, p. 515.
25. Panchenkov, G.M. and Lebedev, V.P., *Khimicheskaya kinetika i kataliz* (Chemical Kinetics and Catalysis), Moscow: Khimiya, 1985.
26. Vityaz', P.A., Sheleg, V.K., Anan'in, V.N., *et al.*, *Dokl. Akad. Nauk BSSR, Ser. Khim.*, 1986, vol. 30, no. 3, p. 240.
27. Tikhov, S.F., Potapova, Yu.V., Fenelonov, V.B., *et al.*, *Kinet. Katal.*, 2003, vol. 44, no. 2, p. 322.
28. Tikhov, S.F., Zaikovskii, V.I., Fenelonov, V.B., *et al.*, *Kinet. Katal.*, 2000, vol. 41, no. 6, p. 916.
29. Anan'in, V.N., Belyaev, V.V., Romanenkov, V.E., *et al.*, *Vestsi Akad. Navuk BSSR*, 1988, no. 5, p. 17.
30. Lur'e, B.A., Chernyshev, A.N., Perova, N.N., *et al.*, *Kinet. Katal.*, 1976, vol. 17, no. 6, p. 1453.
31. Lyashko, A.P., Medvidinskii, A.A., Savel'ev, G.G., *et al.*, *Kinet. Katal.*, 1990, vol. 31, no. 4, p. 967.
32. Rat'ko, A.I., Romanenkov, V.E., Bolotnikova, E.V., and Krupen'kina, Zh.V., *Kinet. Katal.*, 2004, vol. 45, no. 2, p. 299.
33. Tikhov, S.F., Potapova, Yu.V., Sadykov, V.A., *et al.*, *Mater. Res. Innov.*, 2005 (in press).
34. Rat'ko, A.I., Romanenkov, V.E., Bolotnikova, E.V., *et al.*, *Kinet. Katal.*, 2004, vol. 44, no. 1, p. 169.
35. Tikhov, S.F., Sadykov, V.A., Potapova, Yu.V., *et al.*, *Stud. Surf. Sci. Catal.*, 1998, vol. 118, p. 797.
36. Zaporina, N.A. and Lokenbakh, A.K., *Latv. PSR Zinat. Akad. Vestis. Kim. Ser.*, 1987, no. 6, p. 696.
37. Rat'ko, A.I., Romanenkov, V.E., Bolotnikova, E.V., *et al.*, *Vestsi Nats. Akad. Navuk Belarusi, Ser. Kolloidn. Khim.*, 2003, no. 3, p. 5.
38. Ivanova, A.S., Skripchenko, E.V., Moroz, E.M., *et al.*, *Izv. Sib. Otd. Akad. Nauk SSSR, Ser. Khim. Nauk*, 1989, no. 6, p. 116.
39. Koryabkina, N.A., Ismagilov, Z.R., Shkrabina, R.A, *et al.*, *Kinet. Katal.*, 1991, vol. 32, no. 4, p. 1013.
40. Koryabkina, N.A., Litvak, G.S., Shkrabina, R.A., *et al.*, *Kinet. Katal.*, 1993, vol. 34, no. 5, p. 913.
41. Koryabkina, N.A., Shkrabina, R.A., Ushakov, V.A., *et al.*, *Kinet. Katal.*, 1997, vol. 38, no. 1, p. 128.
42. Segalova, E.E., Tulovskaya, Z.D., Brutskus, T.K., *et al.*, *Zh. Prikl. Khim.*, 1964, vol. 37, no. 6, p. 1227.

43. Pavlova, S., Tikhov, S., Sadykov, V., *et al.*, *Stud. Surf. Sci. Catal*, 2004, vol. 147, p. 223.
44. Tikhov, S.F., Fenelonov, V.B., Zaikovskii, V.I., *et al.*, *Microporous Mesoporous Mater.*, 1999, vol. 33, p. 137.
45. Zagrafskaya, R.V., Karnaukhov, A.P., and Fenelonov, V.B., *Kinet. Katal.*, 1979, vol. 20, no. 2, p. 465.
46. Leonov, A.N., Smorygo, O.L., Romashko, A.N., *et al.*, *Kinet. Katal.*, 1998, vol. 39, no. 5, p. 691.
47. Buyanov, R.A. and Krivoruchko, O.P., *Kinet. Katal.*, 1979, no. 3, p. 765.
48. Rat'ko, A.I., Romanenkov, V.E., Bolotnikova, E.V., *et al.*, *Kinet. Katal.*, 2004, vol. 44, no. 1, p. 162.
49. Panova, N.B., *Probl. Upr. Teor. Inf.*, 2001, no. 4, p. 74.
50. Leshko, N.B., *Probl. Upr. Teor. Inf.*, 2001, no. 6, p. 26.
51. Matus, P.P., *Matematicheskoe modelirovanie v biologii i meditsine* (Mathematical Modeling in Biology and Medicine), Minsk, 1997.
52. Kafarov, V.V., *Metody kibernetiki v khimii i khimicheskoi tekhnologii* (Cybernetic Methods in Chemistry and Chemical Engineering), Moscow: Khimiya, 1985.
53. Kuznetsova, L.I., Ananin, V.N., Pashis, A.V., and Belyaev, V.V., *React. Kinet. Catal. Lett.*, 1991, vol. 43, no. 2, p. 545.
54. Tikhov, S.F., Sadykov, V.A., Salanov, A.N., *et al.*, *Mater. Res. Soc. Symp. Proc.*, 1998, vol. 497, p. 121.
55. Tikhov, S.F., Sadykov, V.A., Bobrova, I.I., *et al.*, *Stud. Surf. Sci. Catal.*, 2001, vol. 139, p. 105.
56. Ismagilov, Z.R., Podyacheva, O.Yu., Pushkarev, V.V., *et al.*, *Stud. Surf. Sci. Catal.*, 2000, vol. 130, p. 2759.
57. Tikhov, S.F., Kurkin, V.I., Sadykov, V.A., *et al.*, *Stud. Surf. Sci. Catal.*, 2004, vol. 147, p. 37342.
58. Kuznetsova, L.I., Zaikovskii, V.I., Ziborov, A.V., *et al.*, *React. Kinet. Catal. Lett.*, 1991, vol. 43, no. 2, p. 553.